Since January 2020 Elsevier has created a COVID-19 resource centre with free information in English and Mandarin on the novel coronavirus COVID-19. The COVID-19 resource centre is hosted on Elsevier Connect, the company's public news and information website.

Biosensors and Bioelectronics 219 (2023) 114799

Contents lists available at ScienceDirect

Biosensors and Bioelectronics

journal homepage: www.elsevier.com/locate/bios

Toxicity warning and online monitoring of disinfection by-products in water by electroautotrophic biocathode sensors

Chengmei Liao, Lili Tian **, Ziyuan Wang, Xuemei Zhu, Yilian Han, Tian Li, Xin Wang *

MOE Key Laboratory of Pollution Processes and Environmental Criteria, Tianjin Key Laboratory of Environmental Remediation and Pollution Control, College of Environmental Science and Engineering, Nankai University, No. 38 Tongyan Road, Jinnan District, Tianjin, 300350, China

ARTICLE INFO

Keywords:
Biocathode sensor
Dichloromethane
Trichloromethane
Toxic response
Sensitivity

ABSTRACT

As a result of the 2019 coronavirus pandemic, disinfection byproducts generated by the extensive use of chlorine disinfectants have infiltrated the aquatic environment, severely threatening ecological safety and human health. Therefore, the accurate monitoring of the biotoxicity of aqueous environments has become an important issue. Biocathode sensors are excellent choices for toxicity monitoring because of their special electroautotrophic respiration functions. Herein, a novel electroautotrophic biosensor with rapid, sensitive, and stable response and quantifiable output was developed. Its toxicity response was tested with typical disinfection byproducts dichloromethane, trichloromethane, and combinations of both, and corresponding characterization models were developed. Repeated toxicity tests demonstrated that the sensor was reusable rather being than a disposable consumable, which is a prerequisite for its long-term and stable operation. Microbial viability confirmed a decrease in sensor sensitivity due to microbial stress feedback to the toxicants, which is expected to be calibrated in the future by the standardization of the biofilms. Community structure analysis indicated that *Moheibacter* and *Nitrospiraceae* played an important role in the toxic response to chlorine disinfection byproducts. Our research provides technical support for protecting the environment and safeguarding water safety for human consumption and contributes new concepts for the development of novel electrochemical sensors.

1. Introduction

Since the outbreak of the coronavirus disease in 2019 (COVID-19), a large number of disinfectants have been applied in major medical institutions, in wastewater treatment plants, and in various large venues for disinfection to inhibit the spread and dissemination of the virus (Parveen et al., 2022). The overuse of disinfectants inevitably enters the natural water environment. With the sewage discharge systems into the sewage treatment plant will affect the normal operation of the biochemical treatment units, threatening the ecological balance of the receiving waters. Discharge into rivers and lakes with surface runoff can disrupt water chemical processes and ecological succession patterns, impacting the composition of biological communities and the structure and function of ecosystems (Bradbeer et al., 2020). The most heavily used disinfectant during the epidemic was chlorine-containing disinfectant, a broad-spectrum, high-efficiency oxidant that reacts directly with a variety of organic matter and conventional contaminants in natural waters to produce highly toxic, bioaccumulative, and hazardous chlorine disinfection byproducts (CDBPs) (Jkl et al., 2022). Scientific studies and epidemiological investigations have identified more than 1000 contaminants in chlorine-disinfected waters (Claxton et al., 2008), of which 20 are confirmed carcinogens, 23 are suspected carcinogens, 18 are carcinogenic, and 56 are mutagens.

Trichloromethane is one of the major components of CDBPs (Sfynia et al., 2022), which is classified as a suspected carcinogen by the American Cancer Society as early as 1976 (Keysser C. 1976), and its carcinogenic effects have been confirmed in animals. Dichloromethane is also a typical CDBPs (Takahashi and Morita, 2010), which belongs to the class 2A carcinogens in the list of carcinogens published by the International Agency for Research on Cancer (IARC). The analysis of these two substances in water is usually accomplished by headspace injection gas chromatography (Sun and Yan, 2007), which is complicated to operate, has poor sensitivity, has a long response time and is high in economic costs. In addition, some portable toxic and hazardous gas detectors can be used for the nonquantitative detection of gaseous trichloromethane (Giannoukos et al., 2017). However, few means exist for

** Corresponding author.
* Corresponding author.
E-mail addresses: 595745527@qq.com (L. Tian), xinwang1@nankai.edu.cn (X. Wang).

https://doi.org/10.1016/j.bios.2022.114799
Received 15 July 2022; Received in revised form 19 September 2022; Accepted 8 October 2022
Available online 10 October 2022

monitoring CDBPs in waters online, in situ and in real time. Therefore, the development of highly sensitive and responsive toxicity sensors to provide early warning of CDBPs is urgently needed.

Microbial electrochemical sensors using electroactive biofilms (EABs) as sensing elements have been frequently used in recent years for biotoxicity monitoring in various water environments (Du et al., 2022; Na et al., 2021). These sensors can directly translate changes in microbial metabolic activities into an electrical signal response without any other converters or external power conversions to qualitatively warn of known or unknown toxic substances in waters or even quantitatively characterize their levels (Stein et al., 2011), which is the most obvious advantage of the microbial electrochemical sensors (Chen et al., 2016; Sun et al., 2015). At present, microbial electrochemical toxicity sensors mainly use bioanodes as the sensing elements. The anodic microorganisms are usually anaerobic heterotrophs, which need strictly anaerobic environmental conditions and certain concentrations of organic matter to maintain their metabolic activities. However, for the monitoring of aerobic natural waters with low BOD, additional supplemental organic carbon sources and deaeration are required thereby making these sensors difficult and expensive to operate and potentially causing secondary pollution. Fortunately, aerobic electroautotrophic cathodic microorganisms meet all the requirements to function in natural waters. In 2007, Clauwaert et al., (2007) serendipitously discovered that cathodic biofilms formed using inorganic carbon sources, oxygen, inorganic salts and electrode autotrophic growth can act as oxygen reduction catalysts. The major difference between these and anodic microorganisms is that they are electron-accepting autotrophic respirators (Eddie et al., 2016), which provides a theoretical basis for their use as sensitive elements in novel autotrophic microbial electrochemical sensors. Since autotrophic microorganisms grow in more complex environments and are theoretically more sensitive to feedback from toxic substances than heterotrophic bacteria, a significant increase in the sensitivity of microbial electrochemical biosensors can be achieved, which is highly desirable. In 2017, researchers at Tsinghua University (Jiang et al., 2017) verified the feasibility of using biocathodes as sensing units for the first time, reducing the detection limit of formaldehyde to 0.0005% (the lowest detection limit reported in the literature thus far), which is 80% lower than that of bioanodes, indicating that autotrophic biocathodes as sensing units have natural advantages that cannot be matched by anodes. However, compared with bioanode sensors, studies on biocathode sensors are scarce, and the mechanisms active in biocathode sensors have not been fully elucidated. In addition, the existing biocathode sensors have mostly been designed for the toxicity detection of heavy metal ions (Prévoteau et al., 2019) and formaldehyde (Jiang et al., 2017; Liao et al., 2018b) and no sensors for monitoring CDBPs in water have been reported.

In this study, an electrochemical toxicity sensor with an electroautotrophic biocathode as the sensing element was constructed to warn and monitor the typical CDBPs dichloromethane and trichloromethane, and specific response models were further developed. Correlations between the concentrations of the target toxicants and their response signals were characterized by systematically analysing the main parameters of the sensor, such as the detection limit, sensitivity, attenuation ratio and current loss ratio. Furthermore, long-term operational monitoring was used to analyse the causes of performance degradation of the sensor during application. The reusability of the sensor was verified using repeated toxic shock tests and electrochemical performance measurements. The analysis of microbial mortality and microbial community structure before and after toxic shock elucidated the mechanism of the sensor response to CDBPs and laid a theoretical foundation for the further design of standardized biocathode sensors.

2. Materials and methods

2.1. Activation, operation and maintenance of biocathode sensors

A vertical penetrating flow three-electrode system commonly used in our laboratory was chosen for the biocathode sensors (Fig. S1) (Liao et al., 2018b). A carbon fibre brush with a large specific surface area was used for the working electrode to enrich the cathodic electroautotrophic microorganisms, the counter electrode was a 1 cm^2 Pt sheet, and the reference electrode was Ag/AgCl (4.0 M KCl, 201 mV vs. SHE). Oxygen was supplied by circulating flow aeration at a constant flow rate of 19 ± 1 mL min^{-1}.

For the rapid start-up of the biocathode sensor, acclimated mature cathodic biofilms from MFC reactors (Liao et al., 2018a) were collected as the inoculum. The sensors were fed in recirculating mode, where the cathode electrolyte contained 50 mM phosphate buffer solution (PBS: Na_2HPO_4, 4.576 g L^{-1}; NaH_2PO_4, 2.132 g L^{-1}; NH_4Cl, 0.31 g L^{-1}; KCl, 0.13 g L^{-1}), 12.5 mL L^{-1} trace minerals, 5 mL L^{-1} vitamin solution and 0.94 g L^{-1} $NaHCO_3$. All experiments were conducted at room temperature (25 ± 1 °C).

2.2. Electrochemical tests

The sensors were incubated at an applied cathodic potential of −0.2 V (vs. Ag/AgCl) using a multichannel potentiostat (CHI 1000C, CH Instrument, Shanghai, China), and the current was collected every 100 s using chronoamperometry (Liao et al., 2018b). To analyse kinetic variations in biofilms affected by CDBPs, the electrochemical performances of the biocathode sensors over different periods, including before and after the toxicity tests and after recovery, were investigated by cyclic voltammetry (CV, scan rate: 1 mV s^{-1}) over a potential range from 0.5 to −0.3 V (vs. Ag/AgCl).

2.3. Measurements and calculations of responsivity

Dichloromethane and trichloromethane, as representative CDBPs, were selected as model toxicants for testing the performance of the biocathode sensors. After the successful activation of the biocathode sensor, different concentrations of CDBPs (shown as diluted concentrations) were injected into parallel biocathode sensors. When the response currents no longer decreased over time, the biosensors were washed with fresh electrolyte in a continuous flow mode to completely remove CDBPs residues. A circulating incubation pattern was then applied for sensor maintenance to re-establish a stable baseline current. The above steps were repeated for the different CDBPs toxicity tests to verify the long-term operational stability and multiple replicate availability of the sensors. Each toxicity test was designed with a control that substituted water for the toxicant solution. In addition, preexperiments confirmed that the injection of CDBPs did not lead to changes in conductivity.

The current change (ΔI) and the inhibition ratio (IR) are two of the most commonly used indicators for characterizing sensor performance. The ΔI was defined as the current drop after exposure to a target contaminant and was calculated as $\Delta I = I_b - I_a$, where I_b (A) was the pretesting stable baseline current and I_a (A) was the during-testing stable current. The sensitivity could be derived by fitting ΔI to the toxicant concentration with a suitable model. To eliminate errors in the baseline currents between different reactors, the IR was evaluated and calculated as $IR(\%) = \Delta I / I_b \times 100\%$ (Qi et al., 2021). To calculate the irrecoverable current loss, the concept of the current loss ratio (CLR) was introduced and calculated as $\mathrm{CLR}(\%) = (I_b - I_c)/I_b \times 100\%$, where I_c was the post-testing stable current (Li et al., 2016).

2.4. Sensing element status analysis

Confocal laser scanning microscopy (CLSM, LSM880 with Airyscan, Zeiss, Germany) was used for imaging the cathodic biofilms to

characterize the dead/alive state of the sensing elements in response to CDBPs. Additionally, the autofluorescence of proteins was compared at excitation wavelengths of 340–380 nm and emission wavelengths of 435–485 nm to reflect biofilm activity. A cluster of carbon brush samples was removed from the carrier with a sterile knife and placed in an imaging dish. The samples were then stained with a LIVE/DEAD BacLight Bacterial Viability Kit (L13152, Thermo Fisher Scientific Inc.) for 30 min under dark conditions and rinsed with 50 mM PBS to remove any excess dye. ZEN Black software was used to construct 3D images. The percent viability was calculated using ZEN Blue software by counting pixels.

2.5. Biological analyses

Biofilm samples collected before and after toxicity testing with CDBPs were used for DNA extraction with a Soil Genomic DNA Kit (CW2091S, Com Win Biotech Co. Ltd., Beijing, China). The highly variable V4 region of the 16S rRNA gene was sequenced using Illumina MiSeq in Novogene (Beijing, China). Similarity clustering was performed to annotate OTU sequences to study community succession after multiple toxic shocks to the sensor. The whole-genome functional information of the KEGG database annotated by Uproc and Pauda was mapped to the Silva database for OTU clustering to obtain functional annotation information for tx4fun functional prediction of microbial communities. The dominant species were screened to map symbiotic networks characterizing microbial fitness and species interactions. Sequencing results were statistically visualized by R language. All sequence datasets in this study are available from the NCBI/Sequence Read Archive (SRA) under BioProject accession number PRJNA834921.

3. Results and discussion

3.1. Activation of the biocathode sensors

Biocathode sensors require a long activation period due to the extremely slow growth and reproduction of the cathodic autotrophic bacteria. The time-current curves (Fig. S2) showed an exponential increase in the current of the biocathode sensors with the growth and propagation of electroactive microorganisms after a 24-day retardation period (Liao et al., 2018a). A stable period was reached after another 5 days, and the current exhibited stable fluctuations, indicating the successful domestication of the biocathode sensors with stable baseline currents concentrated at 1.25 ± 0.17 mA.

3.2. Biocathode sensor for dichloromethane concentration determination

Toxicity testing of dichloromethane was performed after baseline currents were stably maintained for 24 h. A decrease in current was observed immediately (<100 s) after dichloromethane injection for each biocathode sensor except for the control, indicating that a typical toxic response in the cathodic microorganisms occurred in the concentration range of 0.05–0.5 mg L^{-1} dichloromethane (Fig. 1A). A current drop of 0.18 mA was induced when 0.05 mg L^{-1} dichloromethane was added, while a 10-fold increase in the concentration of dichloromethane decreased the current by 0.69 mA. The value of ΔI increased with increasing concentrations of dichloromethane addition, which was consistent with the response characteristics of the toxicity sensor. Model fitting showed a linear increase in current attenuation with increasing dichloromethane concentration (R^2 = 0.9838, Fig. 1B). A sensitivity of 1.08 mA mg^{-1} L^{-1} was derived by calculating the slope, indicating that each 1 mg L^{-1} increase in dichloromethane produced a current drop of 1.08 mA. Similarly, the inhibition ratio emerged an excellent linear fit

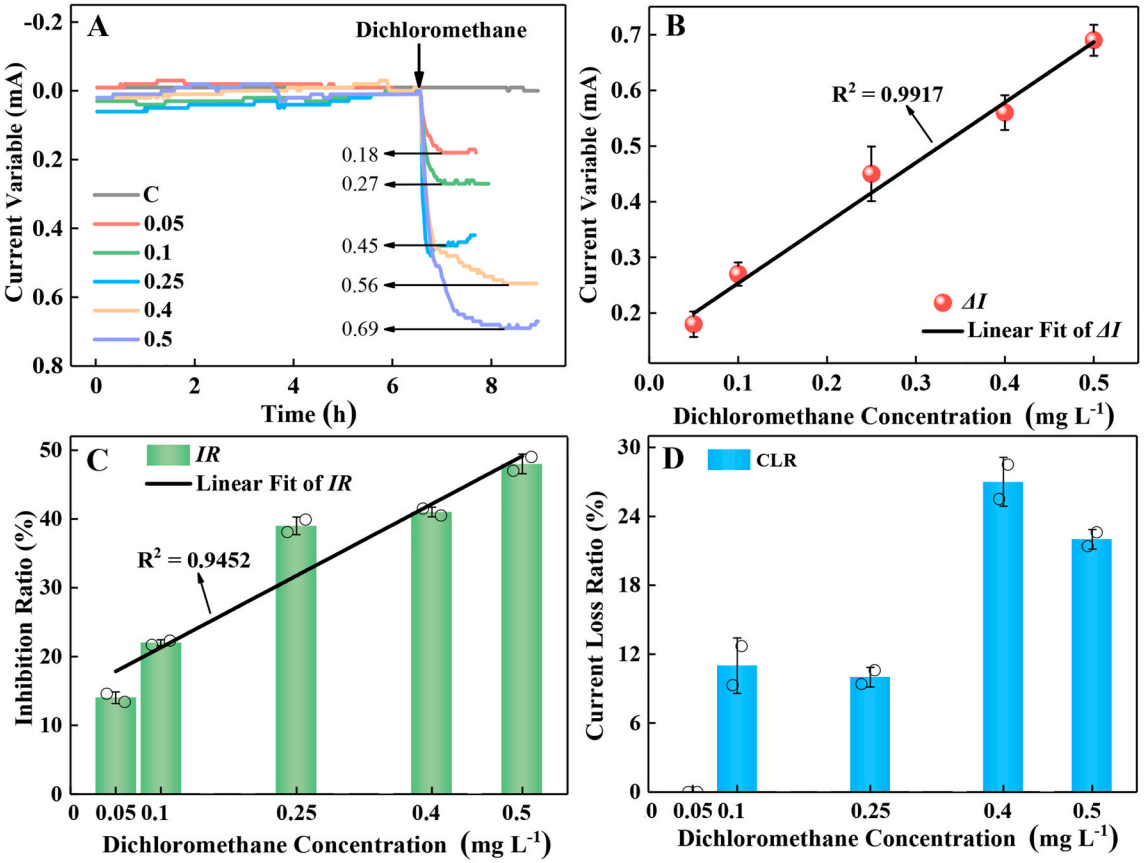

Fig. 1. Current variables (A), response sensitivity (B), inhibition ratio (C) and current loss rate (D) of the biocathode sensor response to dichloromethane.

(R^2 = 0.9452) due to the good baseline current parallelism between sensors, further confirming the high accuracy of the sensor for dichloromethane concentration determination (Fig. 1C). The current loss ratio caused by increasing dichloromethane concentrations increased from 0% to 27%, and the corresponding response time was also prolonged (Fig. S3). For example, the sensor with 0.25 mg L^{-1} dichloromethane needed a response time of 0.3 h to reach a stable current with a CLR of 10 ± 0.8%, whereas the 0.4 mg L^{-1} system required 483% more time (1.75 h) to reach a CLR of 27 ± 2.1%, indicating that the electroautotrophic bacteria gradually failed to recover with increasing concentrations of dichloromethane due to toxic inhibition (Fig. 1D).

3.3. Biocathode sensor for trichloromethane concentration determination

Upon completion of the dichloromethane toxicity tests, the electrolyte was refreshed via a continuous stream for sensor operation and maintenance. After approximately 4 days of repair, the biocathode sensor regained a stable baseline current (2.22 ± 0.32 mA), which was elevated by 78% due to the activation of stress regulation in the cathodic microorganism induced by toxic shock from dichloromethane (Fig. S4). Similarly, as with the determination of dichloromethane, the biocathode sensor responded rapidly after trichloromethane (0.1–0.9 mg L^{-1}) injection except for the control (Fig. 2A and Fig. S5), fitting its current variable to the trichloromethane concentration with a degree of agreement as high as 0.9772 (Fig. 2B). More interestingly, the calculated sensitivity of the biocathode sensor for trichloromethane was also 1.08 mA mg^{-1} L^{-1}, indicating that the toxic inhibition induced by dichloromethane and trichloromethane was very similar, which also revealed this sensor could be used to determine the combined concentration of multiple CDBPs with both dichloromethane and trichloromethane remained in the actual natural water, rather than just acting as a warning equipment. However, the detection ranges of dichloromethane and trichloromethane deviated from each other because their biotoxicity to microorganisms was not exactly the same. Additionally, the results of *IR* (Fig. 2C) and CLR (Fig. 2D) were consistent with those obtained from the testing of dichloromethane, where high concentrations of trichloromethane inhibited the electroactivity of cathodic microorganisms, inducing large current drops and irrecoverable electrical losses. This further confirmed the feasibility of using the sensor for the determination of CDBPs in natural waters.

3.4. Toxic response of biocathode sensors to CDBPs

Toxic CDBPs usually coexist in natural waters. Given the very similar toxic inhibition responses of the cathodic microorganisms by dichloromethane and trichloromethane, combined testing with half the concentration of each of the two toxicants was conducted to study the toxic response of the biocathodic sensor to CDBPs in natural waters. Their concentrations were summed, and the combined concentration gradients were calculated as 0.08, 0.2, 0.3, 0.5 and 0.7 mg L^{-1}. The recovery current of the sensor stabilized at 1.75 ± 0.05 mA (Fig. S6) before the test. As with the previous two toxicity tests, the biocathode sensor continued to respond steadily to changes in the concentration of the combined toxicants (Fig. 3A). However, the current variables induced by the combined concentrations were lower than that of their individual toxic responses. Taking 0.5 mg/L as an example, the current variable (0.34 mA) induced by the combined shock was 50% and 45% lower than that of dichloromethane (0.69 mA) and trichloromethane (0.62 mA) alone, respectively. More intuitively, the sensitivity (0.788 mA mg^{-1} L^{-1}) (Fig. 3B) and *IR* (Fig. 3C) of the biosensor decreased as the number of toxic shocks increased, indicating that the cathode electroactive microorganisms matured and stabilized with the long-term operation of the sensor and that the constant toxic stimuli activated bacterial

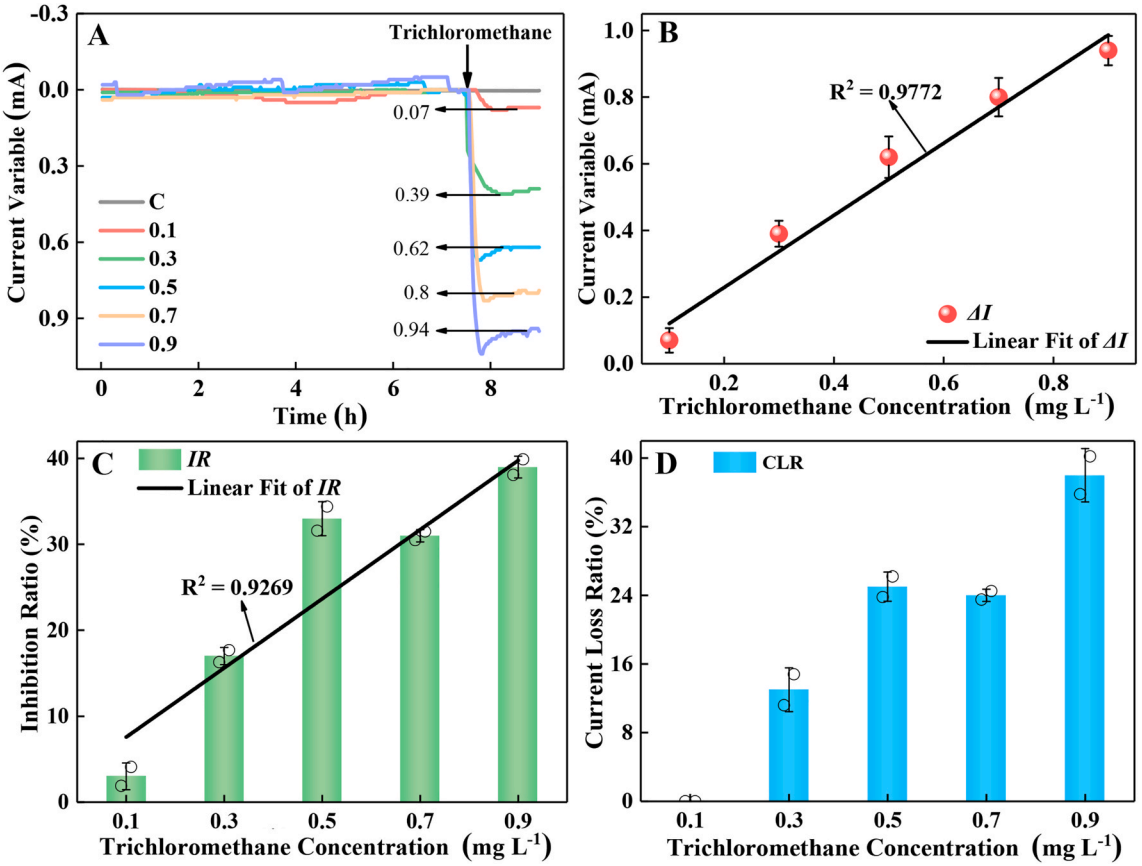

Fig. 2. Current variables (A), response sensitivity (B), inhibition ratio (C) and current loss rate (D) of the biocathode sensor response to trichloromethane.

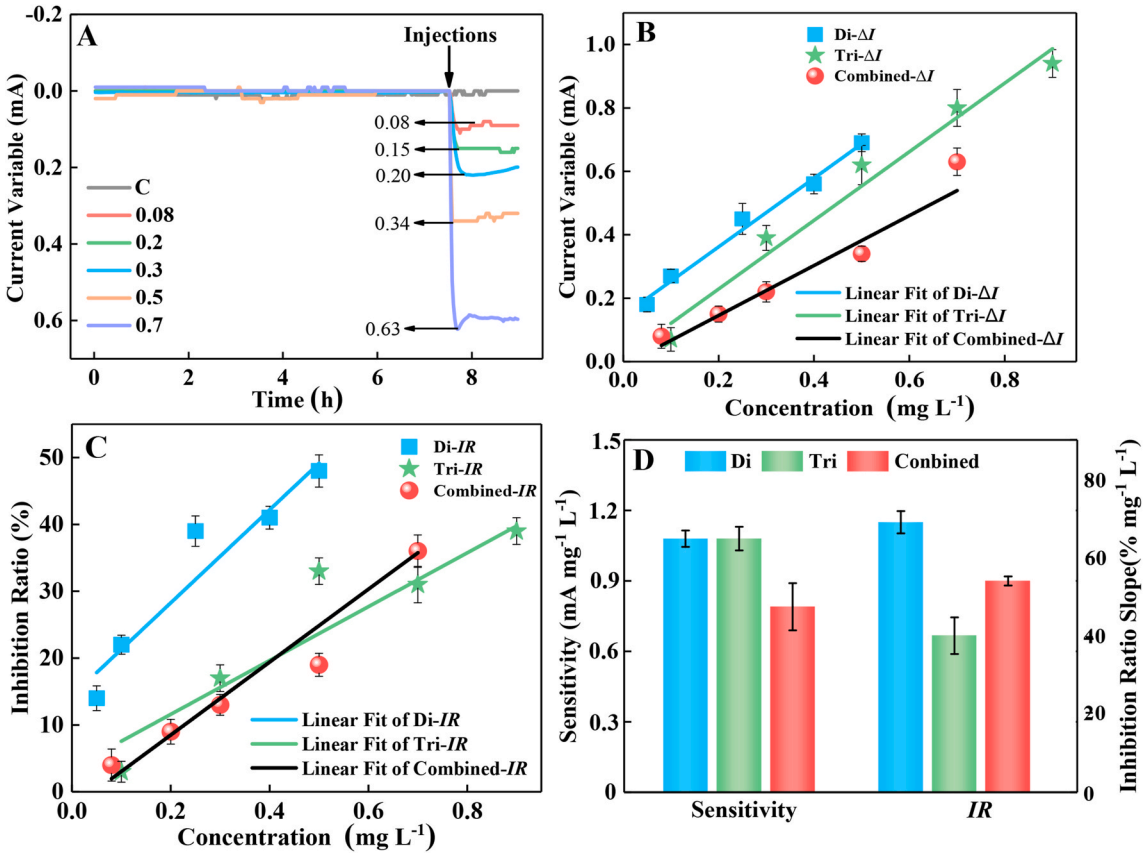

Fig. 3. Current variables (A) of the biocathode sensor response to the combined toxicity of dichloromethane and trichloromethane. Summary of the response sensitivity (B), inhibition ratio (C) and histogram (D) of the biocathode sensor response to three toxic shocks.

resistance (Fig. 3D). This was also reflected well in the CLR, where the current loss ratio caused by 0.5 mg L^{-1} of toxicant decreased from 24% to 8%, demonstrating the increased resistance of the microorganisms and their decreased sensitivity to the oxicants, which is a common drawback of biosensors (Fig. S7C). However, this did not have a significant impact on the accuracy of the sensor in determining toxic concentrations, with the sensitivity and *IR* fit of the sensor for the third test showing values as high as 0.9369 (Fig. S7A) and 0.9873 (Fig. S7B), respectively. And their biases were getting close to 0, which also indicated that the tests were quite accurate. More importantly, the current loss of the stable and mature sensor was reduced, and the early warning response to toxic substances was more rapid and efficient, which laid the theoretical foundation and provided technical support for practical applications.

3.5. *The remediation and reuse of biocathode sensors*

The ability to recover performance after multiple uses and prevent the wastage of "disposable consumables" was one of the most valuable aspects of the sensor. After each completed toxicity test, the biocathode sensor was able to regain a stable baseline current after being refreshed with fresh electrolyte at a continuous flow (Fig. S4). Further, cyclic voltammetry (CV) was applied to the biocathode sensor before and after the toxic test and during the fresh electrolyte maintenance to reveal the mechanism of toxic shock on the biocathode sensor and to verify its recoverability. Upon activation of the biocathode sensor, CV (Fig. 4A) showed characteristic parallel electrochemical "S" curves with two irreversible reduction peaks (0.22 ± 0.03 V and −0.19 ± 0.01 V), whose corresponding peak current densities were 120 ± 2 A/m^3 and 147 ± 6 A/m^3. Similarly, the derivatives of the CV (DCV) curves showed a pair of significant symmetrical main peaks at 0.341 ± 0.006 V and their redox activities were very consistent (Fig. 4B), indicating that the six sets of biocathode sensors had high and parallel electrochemical performances and could be used as parallel sensors for toxicity determination.

The CV curves after toxicity testing showed a current density decay of 39%–53% over the scan range (Fig. 4C), with the greatest decay coming from the sensor with the highest concentration of added toxicants, where the current density at −0.3 V decreased from 156 A m^{-3} to 74.1 A m^{-3}. As the toxicant concentration increased, the shape of the CV curve increasingly deviated from the standard "S" shape, which indicated that the metabolic activities of the cathodic microorganisms that created the sensitive elements of the sensor were inhibited by the disinfection byproducts, resulting in a decrease in the electron transfer capacity. Additionally, DCV (Fig. 4D) presented no shift in the midpoint potential, but the sensor subjected to a high concentration of toxic shock exhibited some scrambled peaks, and the current density of the main peak decreased with increasing toxicant concentration, indicating that the main electrochemically active substances (e.g., oxidoreductase or electron shuttle substances) were not changed, but the toxic shock may have caused feedback regulation of microorganisms to produce some electrochemically active substances such as some electron shuttles or even to dredge some electron transfer pathways.

CV (Fig. 4E) was also performed after recovery from the toxicity testing to further verify sensor reusability. The CV curves of the recovered biocathode sensors displayed improved electrochemical performance compared with those of the toxic shock tests; specifically, the current density at −0.3 V increased to 150 A m^{-3}, which was comparable to the CV curves in the absence of the toxicants, suggesting that the cathodic microorganisms had the ability to recover and resume their metabolic activities after a period of incubation in a suitable environment. In DCV (Fig. 4F), the central potential of the main peak was also not shifted. The sensors that were subjected to low concentrations of

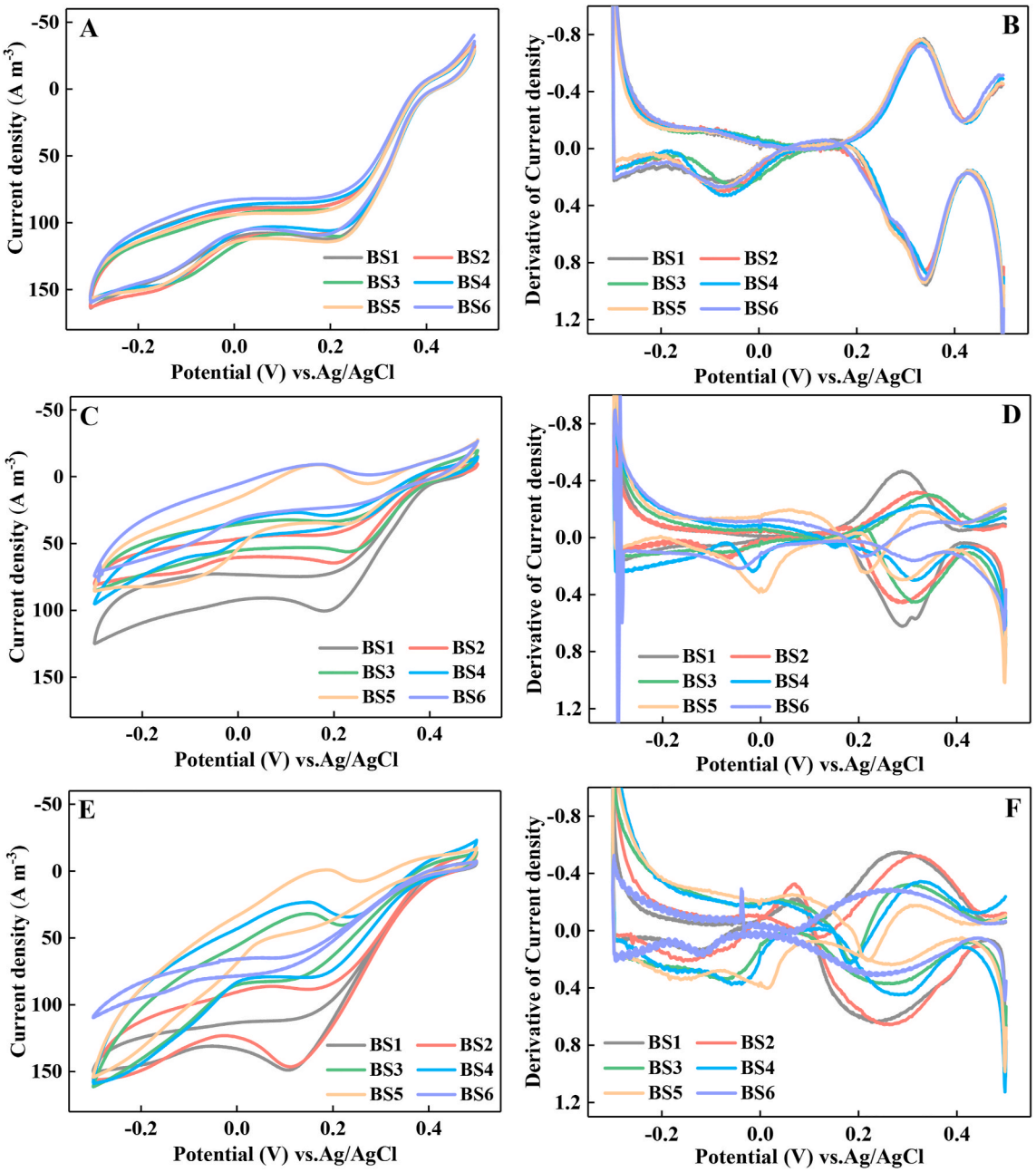

Fig. 4. Electrochemical performance test of the biocathode sensor over different periods. CV (A) and DCV (B) before toxic shock, CV (C) and DCV (D) after the toxic tests and CV (E) and DCV (F) during maintenance with fresh electrolyte. BS1-6 indicated 6 sets of biocathode sensors, respectively.

toxicants almost completely recovered their original electrochemical performance. However, the sensors that were exposed to high concentrations of toxicants showed spurious peaks, which may have been caused by irreversible damage to the cathodic microorganisms under high-toxicity conditions, resulting in changes in their electroactive substances (e.g., electron shuttles) or in changes to redox reactions at the microbe-electrode interface. This was the principle of the sensor response to CDBPs and the reason for the performance degradation after long-term operation.

3.6. Viability of biofilm after the CDBPs test

CLSM images of the biofilms before and after the toxicity tests showed that the survival (Fig. 5A) and metabolic activity (Fig. 5B) of microorganisms were more inhibited with increasing concentrations of CDBPs. The biofilm survival rate after multiple shocks with high concentrations of CDBPs (H) decreased from 95% to 43% (Fig. 5C), which well explained the decrease in sensitivity due to multiple toxicities and the inability of the sensor to fully recover its activity after high-concentration toxicity tests. The toxic electrolyte containing CDBPs made contact with the biofilms on the cathode and stimulated the metabolic activities and mass transfer processes of microorganisms within the biofilms (Shen et al., 2013), thus inhibiting the electron transfer process of the biocathode sensor and leading to a drop in current.

3.7. Microbial community responses

The species diversity, composition, function and symbiotic relationships of microbial communities could be visualized to show the response of the sensor-sensitive elements to the toxic effects of CDBPs. Dilution curves showed a significant increase (by 67%–148%) in species

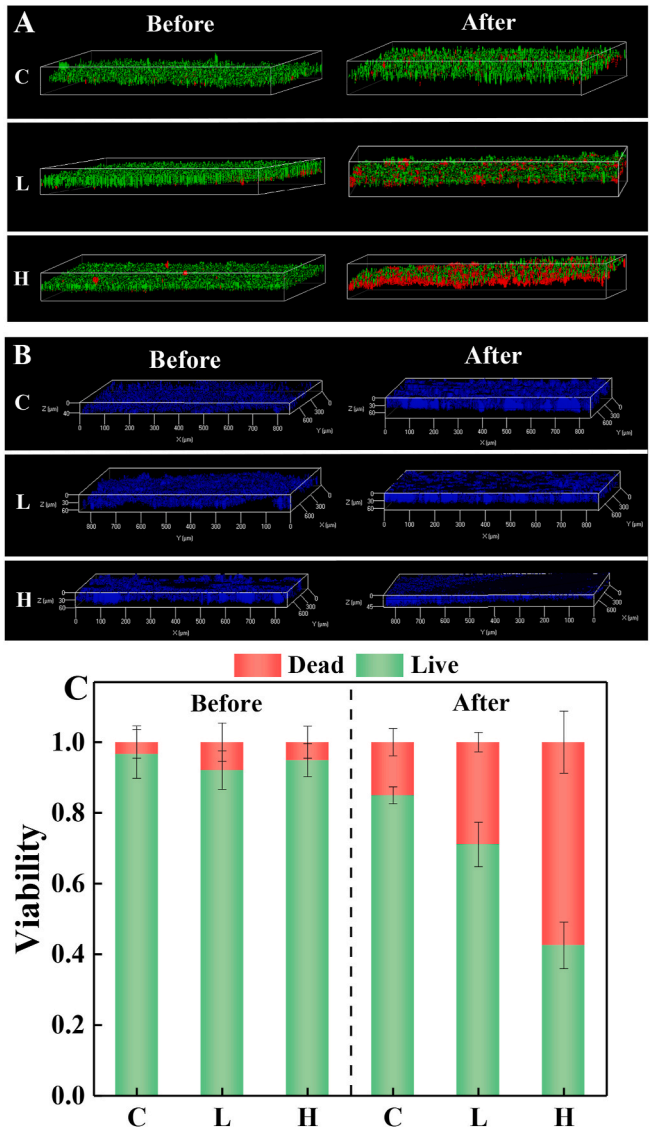

Fig. 5. Stacked CLSM images of the survival (A) and metabolic activities (B) of microorganisms before and after the multiple CDBP toxicity tests, where the green/red and blue were live/dead of bacteria and proteins with auto-fluorescent amino acids, respectively. Viability was calculated by counting pixels (C). C, L, and H represent the control (C) without toxicity testing and the shock group with high (H) and low (L) concentrations of CDBPs, respectively.

richness after multiple tests with CDBPs (Fig. S8) as a result of microbial stress feedback. According to the species annotations, Proteobacteria (59%–71%) was the dominant phylum in the mature cathodic biofilms, consistent with previous findings (Liao et al., 2018a). However, the percentage of this phylum substantially decreased to 15%–30% after the CDBP tests, especially under high CDBP concentrations, whereas the sum of the abundance of Bacteroidetes, Nitrospirae, and Acidobacteria simultaneously increased from 7.2%–17%–52%–68%, with a 3–7.6-fold increase (Fig. S9A).

Further annotation at the genus level significantly highlighted the abundance of *Moheibacter* (from 0.04%–0.17%–16%–32%) belonging to Bacteroidetes, followed by *Nitrospiraceae* (from 2.5%–14%–9.2%–27%) belonging to Nitrospirae, while other genera, such as *Pseudofulvimonas*, *Hydrogenophaga*, and *Nitrosomonas* belonging to Proteobacteria decreased (Fig. 6A), which is in good agreement with the results at the phylum level (Fig. S9B). The differential OTUs (Fig. 6B) observed after multiple toxicity tests positively correlated with the increase in CDBP concentrations (Fig. S10A), revealing that microorganisms responded to the CDBPs by forming their own community-specific genera while gradually increasing their resistance to the external environmental disturbance.

Intergroup variability contribution analysis further highlighted the importance of *Moheibacter* and *Nitrospiraceae* (Fig. 6C and Fig. S10B), which played a vital role in the sensor response to the CDBPs. *Moheibacter* is a yellow, rod-shaped, strictly aerobic, nonmotile Gram-negative bacterium whose cellular peroxidase positivity is extremely viable during two-electron oxygen reduction. In addition, studies (Liu et al., 2021) have shown its resistance to various antibiotics, such as ceftriaxone, penicillin and kanamycin, as well as the presence of genes associated with copper homeostasis in the genome, suggesting that this strain has a strong potential to compete with other microorganisms. *Nitrospiraceae* is a well-reported cathodic electroactive bacterium (Garcíamuñoz et al., 2011; Wu et al., 2017), whose autotrophic nitrite oxidation function (Daims et al., 2001) in denitrifying biocathodes (Kelly and He, 2014) can promote power production while synergizing nitrogen metabolism with other denitrifying bacteria (such as *Nitrosomonas*) (Liao et al., 2018a). The substantial enrichment of this bacterium after CDBP testing suggested that long-term operation and external environmental disturbances can stimulate the potential of highly active cathodic bacteria, which further explained the intrinsic reasons for the improved electrochemical performance as well as for the decrease in sensitivity in the sensors after repeated CDBP exposure.

Symbiotic networks among microorganisms reflect the adaptability of microorganisms and interactions between dominant species (Fig. 6D). The microbial community relationships before toxicity testing were relatively simple, with antagonistic relationships formed by the *Parvibaculum*, *Arcobacter*, *Nocardia*, and *Comamonas* camps and the *Acinetobacter* and *Nitrosomonas*-dominated camps. In contrast, the microbial communities after toxicity testing became extremely complex in terms of interspecific relationships as species diversity increased. While the main relationships were still divided into two camps, the rise in the abundance of *Moheibacter* and *Nitrospiraceae* complicated the competitive and cooperative relationships between species, which was a stress-induced feedback response to the CDBPs. Although the community composition and relationships after exposure to CBDPs evolved significantly after toxicity testing, evidently their main functions did not change, with up to 6063 common functions and almost no unique functions highlighted in each sensor (Fig. S11A), which was the basis for their long-term stable operation and reusability as sensors. The functions of the Top20 (Fig. S11B) were mainly related to the N cycle metabolism, and this was in good agreement with the community composition results of the species.

4. Conclusion and outlook

Dichloromethane and trichloromethane are typical CDBPs, and high residual concentrations of these compounds can be very harmful, so real-time monitoring is required to ensure the safety of treated waters. This study systematically investigated the toxicity response of MEC sensors with electroautotrophic bacteria as the sensitive components to dichloromethane, trichloromethane and the combination of the two CDBPs in water. Once the target toxicants were introduced, the current of the biocathode sensors immediately decreased, and the variables of the current was highly and linearly correlated with the concentration of the toxicants, with a fit of 0.9917 for dichloromethane and up to 0.9772 for trichloromethane. More interestingly, the biosensor had the same response sensitivity (1.08 mA mg^{-1} L^{-1}) to dichloromethane and trichloromethane toxicity, indicating that both the CDBPs have the same inhibitory effect on the cathodic electroautotrophic microorganisms, which allows for the testing of combined toxicity responses. The combined toxicity tests revealed a decrease in sensor sensitivity, which was confirmed by microbial survival and community structure analyses to be due to long-term operation and microbial stress feedback to the toxicants, a common phenomenon in biosensors. This limitation is expected

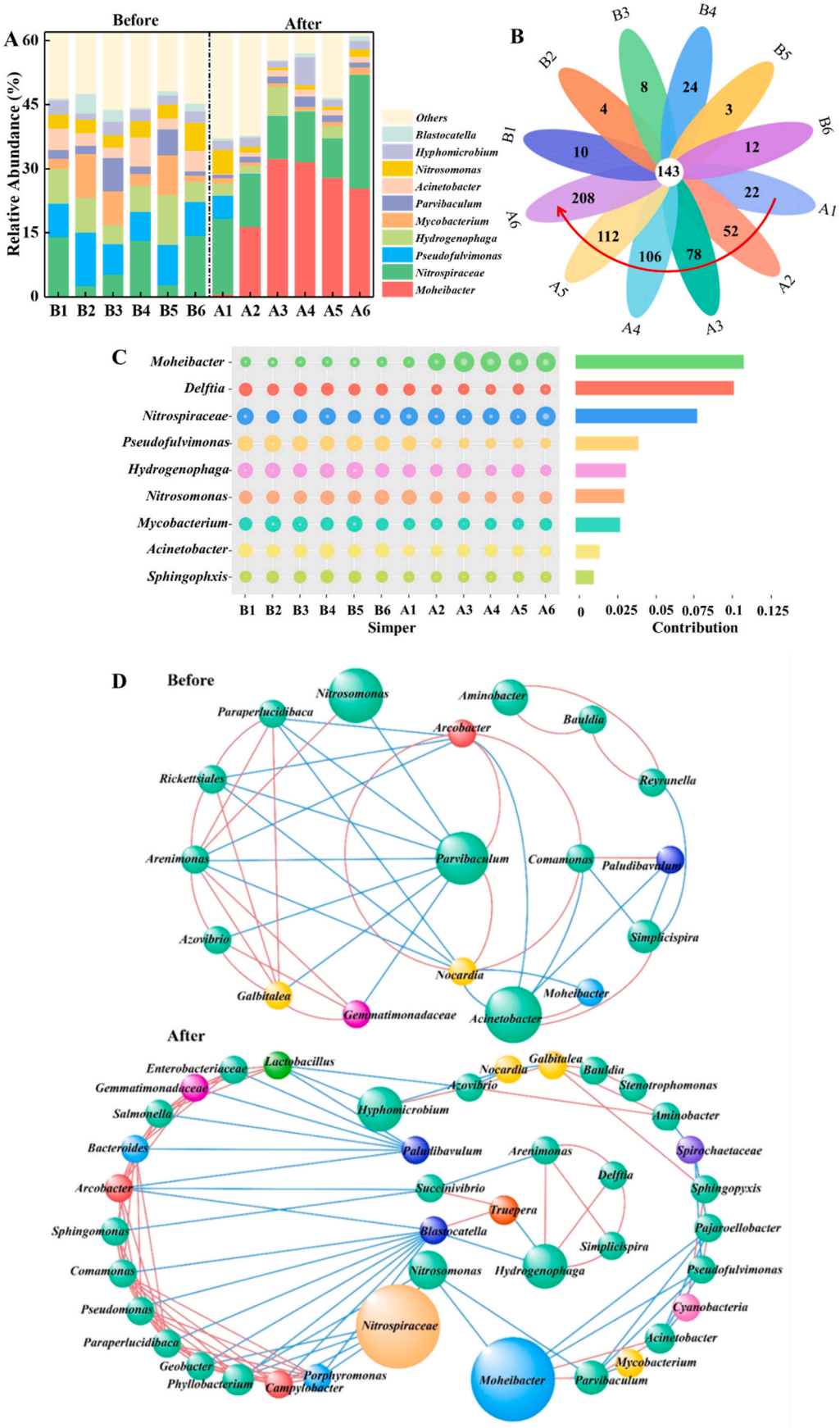

Fig. 6. Relative abundance (A) of bacterial communities at the genus level, Venn diagram (B) of the common and unique OTUs among different samples and the similarity percentage (C) of biocathode communities at the genus level. Symbiotic networks with genus-level correlation coefficients (D). Correlation coefficients for valid associations were greater than 0.1 or less than −0.1 and significant (p value less than 0.05). The different colours represent the different phylum levels. Red represents positive correlations, the blue dashed lines represent negative correlations, and "before" and "after" indicate biofilm samples before and after multiple CDBP tests, respectively.

to be overcome by the standardization of biofilms in the future. Current recovery after toxic shock and CV testing of the sensor for different periods of time verified its reusability. Microorganisms inhibited by low concentrations of CDBPs could fully recover their electrical activity after incubation with a fresh electrolyte solution, but high concentrations of toxic substances produced nonrecoverable attenuation of the current, which indicates that a threshold of tolerance exists for the cathodic microbial sensor to CDBPs and suggests that the performance degradation of sensitive elements during the long-term operation of the sensor needs to fully considered and corrected for deviations in a timely manner. In addition, the presence of potential interferents such as cationic surfactants may affect the application of the sensor in the actual water environment, and further corrections to the model are required. For further practical applications, a target detection range of 0.1–1.0 mg L^{-1} is considered, and the water are first pretreated accordingly to enable them to be within our detection range. For example, for lower concentrations, appropriate evaporation concentration can be applied, while higher concentrations are diluted.

CRediT authorship contribution statement

Chengmei Liao: Designed the experiments, Performed the experiments, Formal analysis, Methodology, Investigation, and Writing. **Lili Tian:** Discussion, Supervision, and Editing. **Ziyuan Wang:** Data curation, and . **Xuemei Zhu:** Methodology, and Discussion. **Yilian Han:** Experiment and, Methodology. **Tian Li:** Designed the experiments and Discussion. **Xin Wang:** Designed the project, Designed the experiments, Writing – original draft, and .

Declaration of competing interest

The authors declare that they have no known competing financial interests or personal relationships that could have appeared to influence the work reported in this paper.

Data availability

All sequence datasets in this study are available from the NCBI/Sequence Read Archive (SRA) under BioProject accession number PRJNA834921.

Acknowledgements

This research work was financially supported by National Natural Science Foundation of China (No. 52100048), the Postdoctoral Science Foundation of China (Nos.2020M680866), the National Natural Science Foundation of China (Nos. 51922051 and 52270042) and the Ministry of Education of China (T2017002).

Appendix A. Supplementary data

Supplementary data to this article can be found online at https://doi.org/10.1016/j.bios.2022.114799.

References

Bradbeer, S.J., Coughlan, N.E., Cuthbert, R.N., 2020. The effectiveness of disinfectant and steam exposure treatments to prevent the spread of the highly invasive killer shrimp,Dikerogammarus villosus. Sci Rre-UK 10 (1), 1919.

Chen, Z., Ling, Z., Niu, Y., Liu, P., Khan, A., 2016. A novel biosensor for p-nitrophenol based on an aerobic anode microbial fuel cell. Biosens. Bioelectron. 85, 860–868.

Clauwaert, P., Ha, D.V.D., Boon, N., Verbeken, K., Verstraete, W., 2007. Open air biocathode enables effective electricity generation with microbial fuel cells. Environ. Sci. Technol. 41 (21), 7564–7569.

Claxton, L.D., Pegram, R., Schenck, K.M., Simmons, J.E., Warren, S.H., 2008. Integrated disinfection by-products research: Salmonella mutagenicity of water concentrates disinfected by chlorination and ozonation/postchlorination. J. Toxicol. Environ. Health A 71 (17), 1187–1194.

Daims, H., Nielsen, J.L., Nielsen, P.H., Schleifer, K.H., Wagner, M., 2001. In situ characterization ofNitrospira-like nitrite-oxidizing bacteria active in wastewater treatment plants. Appl. Environ. Microbiol. 67 (11), 5273–5284.

Du, L., Yan, Y., Li, T., Liu, H., Li, N., Wang, X., 2022. Machine learning enables quantification of multiple toxicants with microbial electrochemical sensors. ACS EST Engg. 2 (1), 92–100.

Eddie, B.J., Tender, L.M., Lin, B., Malanoski, A., 2016. Toward understanding long-distance extracellular electron transport in an electroautotrophic microbial community. Energy Environ. Sci. 9 (11), 3544–3558.

Garcíamuñoz, J., Amils, R., Fernández, V., Lacey, D.A., Malki, M., 2011. Electricity generation by microorganisms in the sediment-water interface of an extreme acidic microcosm. Int. Microbiol.Offc. J.Spanish Soc. Microbiol. 14 (2), 73–81.

Giannoukos, S., Joseph, M.A., Taylor, S., 2017. Portable mass spectrometry for the direct analysis and quantification of volatile halogenated hydrocarbons in the gas phase. Anal. Methods 9 (6), 910–920.

Jiang, Y., Liang, P., Liu, P., Wang, D., Miao, B., Huang, X., 2017. A novel microbial fuel cell sensor with biocathode sensing element. Biosens. Bioelectron. 94, 344–350.

Jkl, A., Yao, L.A., Zms, A., Bei, Y.A., Qywa, B., Hyh, B., 2022. Effects of chlorine dose on the composition and characteristics of chlorinated disinfection byproducts in reclaimed water. Sci. Total Environ. 824, 153739.

Kelly, P.T., He, Z., 2014. Nutrients removal and recovery in bioelectrochemical systems: a review. Bioresour. Technol. 153 (2), 351–360.

Keysser, C.H., 1976. Report on carcinogenesis bioassay of chloroform. Toxicol. Pathol. 4 (4), 21–22.

Li, T., Wang, X., Zhou, L.A., An, J.K., Li, J.H., Li, N., Sun, H.W., Zhou, Q.X., 2016. Bioelectrochemical sensor using living biofilm to in situ evaluate flocculant toxicity. ACS Sens. 1 (11), 1374–1379.

Liao, C.M., Wu, J.L., Zhou, L.A., Li, T., An, J.K., Huang, Z.L., Li, N., Wang, X., 2018a. Repeated transfer enriches highly active electrotrophic microbial consortia on biocathodes in microbial fuel cells. Biosens. Bioelectron. 121, 118–124.

Liao, C.M., Wu, J.L., Zhou, L.A., Li, T., Du, Q., An, J.K., Li, N., Wang, X., 2018b. Optimal set of electrode potential enhances the toxicity response of biocathode to formaldehyde. Sci. Total Environ. 644, 1485–1492.

Liu, Y., Chang, Y.-Q., Wang, C.-N., Ye, M.-Q., Wang, M.-Y., Du, Z.-J., 2021. Moheibacter lacus sp. nov., isolated from freshwater lake sediment. Curr. Microbiol. 78 (5), 2160–2164.

Na, C.A., Jc, A., Zl, A., Yu, G.A., Ql, A., Wen, H.B., Pl, C., Yong, J., Rjz, A., 2021. Indicators of water biotoxicity obtained from turn-off microbial electrochemical sensors. Chemosphere 286, 131725.

Parveen, N., Chowdhury, S., Goel, S., 2022. Environmental impacts of the widespread use of chlorine-based disinfectants during the COVID-19 pandemic. Environ. Sci. Pollut. Res. 699, 1–19.

Prévoteau, A., Clauwaert, P., Kerckhof, F.M., Rabaey, K., 2019. Oxygen-reducing microbial cathodes monitoring toxic shocks in tap water. Biosens. Bioelectron. 135, 115–121.

Qi, X., Wang, S.Y., Jiang, Y., Liu, P.P., Li, Q.C., Hao, W., Han, J.B., Zhou, Y.X., Huang, X., Liang, P., 2021. Artificial electrochemically active biofilm for improved sensing performance and quickly devising of water quality early warning biosensors. Water Res. 198, 117164.

Sfynia, C., Bond, T., Kanda, R., Templeton, M.R., 2022. Simultaneous prediction of trihalomethanes, haloacetic acids, haloacetonitriles and haloacetamides using simulated distribution system tests. Environ. Sci. Water Res. Technol. 8, 742–756.

Shen, Y., Wang, M., Chang, I.S., Ng, H.Y., 2013. Effect of shear rate on the response of microbial fuel cell toxicity sensor to Cu(II). Bioresour. Technol. 136, 707–710.

Stein, N.E., Keesman, K.J., Hamelers, H.V.M., Straten, G.V., 2011. Kinetic models for detection of toxicity in a microbial fuel cell based biosensor. Biosens. Bioelectron. 26 (7), 3115–3120.

Sun, J.-Z., Kingori, G.P., Si, R.-W., Zhai, D.-D., Zhi-Hong, 2015. Microbial fuel cell-based biosensors for environmental monitoring: a review. Water Sci. Technol. 71 (6), 801.

Sun, S.P., Yan, L.I., 2007. Determination of five kinds halogenated alkane hydrocarbon in drinking water with headspace gas chromatography. J. Environ. Health 24, 723–725.

Takahashi, Y., Morita, M., 2010. Halogenated disinfection by-products in tap water. J. Environ. Chem. Eng. 8 (3), 455–464.

Wu, J.L., Chen, W.S., Yan, Y.Q., Gao, K.L., Liao, C.M., Li, Q., Wang, X., 2017. Enhanced oxygen reducing biocathode electroactivity by using sediment extract as inoculum. Bioelectrochemistry 117, 9–14.